Journal of Orthopaedic Surgery and Research

RESEARCH

Open Access

^{18}F-fluoride PET/CT as an early predictor of bony fusion after posterior lumbar interbody fusion– a prospective study

Marloes J. M. Peters[1], Roel Wierts[2], Elisabeth M. C. Jutten[1], Wouter A. M. Broos[3], Mariel P. ter Laak[4] and Paul C. Willems[1*]

Abstract

Purpose Posterior Lumbar Interbody Fusion (PLIF) is a surgical procedure in which stabilization of spinal segments is achieved by inserting interbody cages filled with bone graft. Positron Emission Tomography (PET) is an imaging modality to assess physiological processes at cellular level, well before manifestation of morphological changes on computed tomography (CT). The goal was to determine whether ^{18}F-fluoride PET/CT findings six weeks after PLIF, can predict bony fusion one year postoperatively on CT.

Materials and methods 20 consecutive PLIF patients (21 levels) were prospectively included. Based on diagnostic CT one year postoperatively, operated segments were classified as pseudarthrotic or fused. ^{18}F-fluoride PET/CT scanning was performed at six weeks and one year, yielding parameters related to overall bone metabolism, bone blood flow and bone mineral incorporation. Differences in PET parameters between groups and follow-up moments were assessed. The area under the curve from the receiver operating characteristic was calculated for each PET parameter as a measure of diagnostic accuracy.

Results 11 segments were classified as pseudarthrotic and 10 as fused. Pseudarthrotic segments showed lower intervertebral overall bone metabolism values compared to fused segments at six weeks. Pseudarthrotic segments showed lower intervertebral bone blood flow at six weeks and lower intervertebral bone mineral incorporation at one year compared to fused segments. Overall bone metabolism of the operated intervertebral disc space at six weeks had the highest diagnostic accuracy for predicting the fusion status at one year.

Conclusions ^{18}F-fluoride PET/CT six weeks after PLIF provides prognostic information on bony fusion at one year.

Keywords ^{18}F-fluoride PET/CT, Spinal fusion, Bone graft, Bone metabolism, Kinetic modelling

*Correspondence:
Paul C. Willems
p.willems@mumc.nl
[1]Department of Orthopaedic Surgery, Maastricht University Medical Center, Maastricht, The Netherlands
[2]Department of Nuclear Medicine and Radiology, Maastricht University Medical Center, Maastricht, The Netherlands
[3]Department of Nuclear Medicine, Albert Schweitzer Ziekenhuis, Dordrecht, The Netherlands
[4]Department of Neurosurgery, Maastricht University Medical Center, Maastricht, The Netherlands

© The Author(s) 2025. **Open Access** This article is licensed under a Creative Commons Attribution-NonCommercial-NoDerivatives 4.0 International License, which permits any non-commercial use, sharing, distribution and reproduction in any medium or format, as long as you give appropriate credit to the original author(s) and the source, provide a link to the Creative Commons licence, and indicate if you modified the licensed material. You do not have permission under this licence to share adapted material derived from this article or parts of it. The images or other third party material in this article are included in the article's Creative Commons licence, unless indicated otherwise in a credit line to the material. If material is not included in the article's Creative Commons licence and your intended use is not permitted by statutory regulation or exceeds the permitted use, you will need to obtain permission directly from the copyright holder. To view a copy of this licence, visit http://creativecommons.org/licenses/by-nc-nd/4.0/.

Introduction

Posterior Lumbar Interbody Fusion (PLIF) is a surgical procedure to stabilize spinal segments by pedicle screw instrumentation and interbody cages filled with bone graft. The intended outcome is definite bony fusion of the vertebrae involved. The failure rate of lumbar spinal fusion is reported between 30 and 46% [1] and non-union or pseudarthrosis is thought to be the cause of pain in a significant number of PLIF patients with persisting or recurrent symptoms [2, 3].

Commonly used imaging modalities for follow-up of PLIF patients are plain radiography and computed tomography (CT) [4]. Radiography and CT aim to visualize callus formation and bony bridging between the involved vertebrae. Since these morphological signs of fusion occur late in the normal course of bone healing, radiography and CT are of limited use in the early postoperative phase [5, 6].

The nuclear imaging modality Positron Emission Tomography (PET) is able to assess physiological processes at a cellular level, well before manifestation of morphological changes [7]. PET/CT with the bone seeking tracer ^{18}F-fluoride enables localization and quantification of bone metabolism. The uptake mechanism of ^{18}F-fluoride is based on ion exchange with the hydroxyl group of hydroxyapatite. The portion of bone crystal that is accessible to blood is available for ^{18}F-fluoride ion exchange [8]. Increased uptake of fluoride is thus related to an increase in bone blood flow and/or an increase in the exposed bone crystal surface [8, 9].

Besides visual inspection, PET/CT scans can be analyzed by full pharmacokinetic modelling [10], yielding the fluoride bone influx rate Ki which correlates with histomorphometric parameters of bone formation [11, 12], as well as parameters related to regional bone blood flow and bone mineral incorporation [13]/osteoblastic activity [14, 15]. As an alternative, the standardized uptake value (SUV) can be used. SUV is a semi-quantitative measure for bone metabolism that is more easily obtained. However, SUV is affected by tracer competition and blood clearance, while Ki is not [16].

We hypothesize that bone metabolism parameters obtained from ^{18}F-fluoride PET/CT scans early after PLIF, can provide prognostic information on the fusion outcome later on. The purpose of this study was to determine whether ^{18}F-fluoride PET/CT findings six weeks after PLIF can predict bony fusion one year postoperatively on CT.

Materials and methods

Patients

A consecutive cohort of 20 patients was prospectively enrolled at the Maastricht University Medical Center between October 2011 and January 2014 after screening 86 potentially eligible patients (Fig. 1). Table 1 shows the patient demographics. One patient underwent PLIF at two levels. Therefore, the number of operated segments was 21. All included patients were operated as in standard care in the Maastricht University Medical Center. Pedicle screw instrumentation (CD Legacy®, Medtronic, Memphis, USA) was inserted at the intended level to ensure primary stabilization. Two Capstone® PEEK cages (Medtronic, Memphis, USA) filled with autologous bone of the local lamina were inserted in the excised vertebral disc space, right and left of the midline. The remaining disc space was packed with autologous bone chips from the laminectomy. Dynamic and static ^{18}F-fluoride PET/CT scans were made at six weeks and one year postoperatively as part of the study protocol. The study was performed in accordance with the Helsinki Declaration of 1975, as revised in 2013, and was approved by the medical ethical committee of the Maastricht University Medical Center (NL.32881.068.11). All subjects signed an informed consent form.

PET and CT images were acquired with an integrated PET/CT scanner (Gemini TF 64 PET-CT, Philips, the Netherlands). After a low-dose CT acquisition (120 kV, 30 mAs, slice thickness 4 mm), dynamic PET scanning started simultaneously with intravenous injection of Na-(^{18}F)-fluoride (mean 194.9 MBq, range 100-221.6 MBq at six weeks; mean 199.9 MBq, range 146-219.8 MBq at one year) and involved a 30-minute list-mode scan of the lower spine (18 cm axial field-of-view). The list-mode scan was rebinned into consecutive time frames: 6×5s, 3×10s, 9×60s, 10×120s. One hour after tracer administration, another low-dose CT was acquired, followed by a static PET scan of two bed positions lasting five minutes each. PET images were reconstructed into CT based attenuation corrected images. At one year follow-up, a diagnostic CT scan (64-slice helical, 120 kV, 250 mAs, slice thickness 1 mm, increment 0.8 mm) was added to the protocol. Scans were viewed on clinical software (EBW, Philips, the Netherlands) and further analyzed on a research tool (PMOD 3.0, PMOD Technologies Ltd, Zürich).

Interbody fusion scoring on CT

Interbody fusion was scored on diagnostic CT one year postoperatively as either 0, 1 or 2, according to the number of bony bridges between the operated vertebrae (Fig. 2.) as previously described [17]. A bony bridge was defined as bone mass progressing from one endplate to the other without interruptions. Scoring was performed by three independent blinded observers (experienced musculoskeletal radiologist RW, experienced nuclear medicine physician BB, junior nuclear medicine physician WB). After consensus was reached, segments were

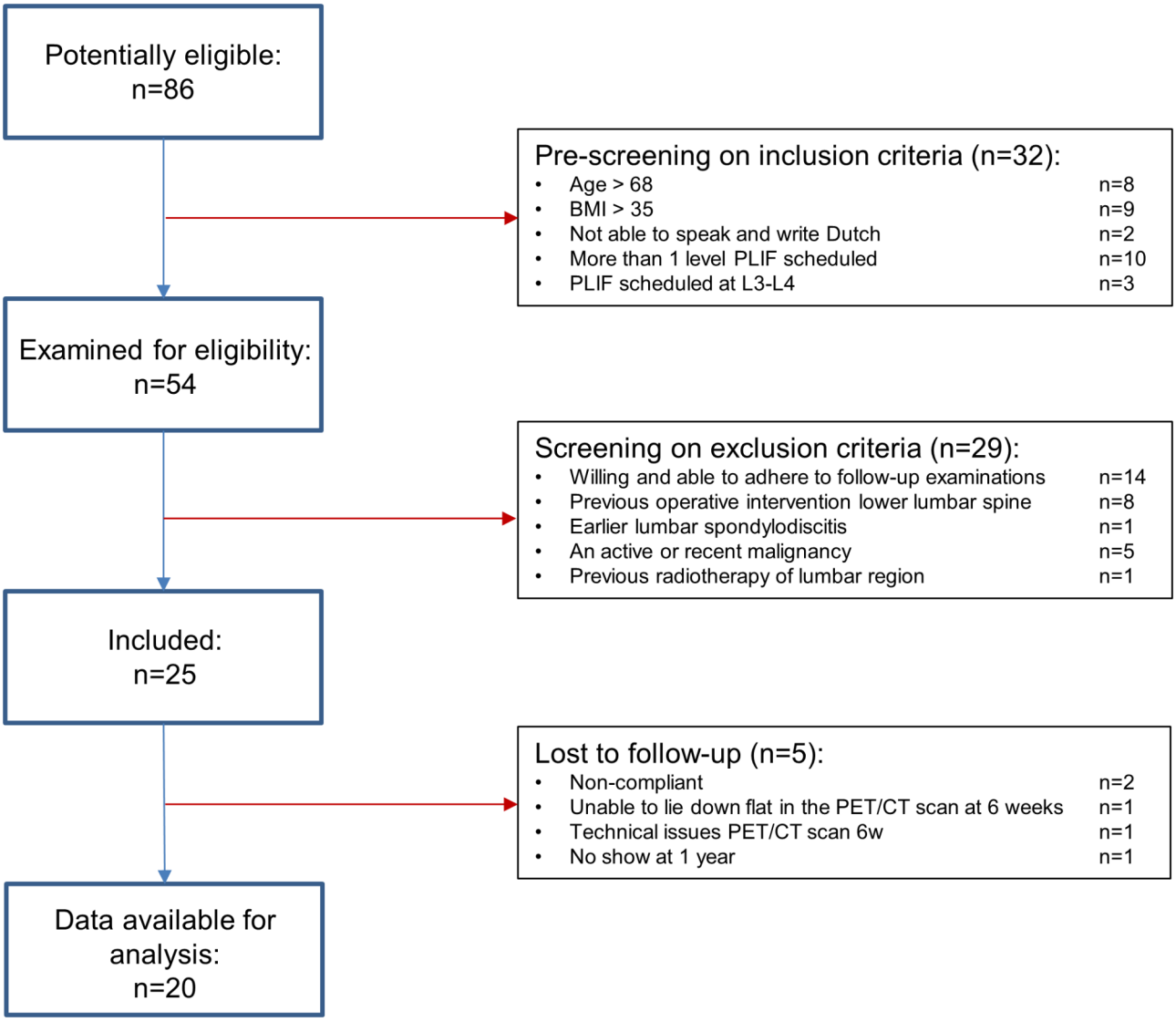

Fig. 1 Flow diagram of the patient selection process indicating reasons and numbers for non-participation at each stage. 86 patients were considered potentially eligible. After pre-screening based on inclusion criteria, the 54 remaining patients were further examined for eligibility by screening based on exclusion criteria. 25 patients were included in the study of which 20 completed the study protocol

classified into either the pseudarthrosis group (score 0) or the fusion group (score 1 and 2).

Analysis of ^{18}F-fluoride PET/CT scans

PET parameters were calculated based on a region of interest (ROI) approach as previously reported [16], by two independent and blinded observers (BB, junior researcher with experience in analyzing PET/CT scans MP). For each low-dose CT, six ellipsoid shaped ROIs were manually drawn following the contours of the vertebrae, including the intervertebral disc space and both endplates of the operated segment (referred to as inter, endUP, endLOW) as well as of a control segment two levels above the operated segment (referred to as inter_C, endUP_C, endLOW_C).

For static analysis, the ROIs were transferred to the static PET image to obtain the maximum SUV (SUVmax [-]) within each ROI, by correcting the measured radioactivity concentration (A [kBq/ml]) for the injected dose of ^{18}F-fluoride (ID [MBq]) and the body weight of the patient (m [kg]) according to [1].

$$SUVmax = \max\left(\frac{A}{ID/m}\right) \quad (1)$$

For dynamic analysis, the ROIs were applied to the dynamic frames to generate tissue time-activity curves (TACs). The arterial input function was determined by an image derived input function (IDIF) [16]. The IDIF and ROI TACs were fitted to the 2-tissue compartment model

Table 1 Patient demographics

Gender	Male (*n* = 13), female (*n* = 7)
Age at surgery	51.7 ± 13.1 years (18–67)
BMI	27.2 ± 2.67 kg/m^2 (21.6–31.3)
Indication	Low grade lumbar spondylolisthesis (*n* = 20)
Level operated	L4-L5 (*n* = 9), L5-S1 (*n* = 12)
Time interval PLIF– early PET/CT (6 weeks)	6.4 ± 0.62 weeks (5.7–8.1)
Time interval PLIF– late PET/CT (1 year)	53.3 ± 3.5 weeks (47.1–61.1)

BMI = body mass index

PLIF = posterior lumbar interbody fusion

PET = positron emission tomography

CT = computed tomography

*mean ± standard deviation (range)

^{18}F-fluoride PET/CT scans

[10, 16], to obtain rate constants K1, k2 and k3. K1 and k2 describe the forward and reverse capillary transport. k3 describes the binding of ^{18}F-fluoride to the bone matrix [18]. The rate constants were combined into Ki, K1/k2 and k3/(k2 + k3) for further analysis. Ki represents the net transport of ^{18}F-fluoride into bone and is a marker for regional *bone metabolism* [10, 11, 19], calculated according to [2].

$$K_i = \frac{K_1 \cdot k_3}{k_2 + k_3} \quad (2)$$

K1/k2 represents the volume of distribution of tracer in the unbound pool [20] and is related to *bone blood flow*. k3/(k2 + k3) represents the fraction of tracer in the extravascular tissue space that undergoes specific binding to the bone mineral [21] and is thus related to *bone mineral incorporation*.

Statistical analysis

Statistical evaluation was performed using IBM SPSS Statistics version 23.0 (Armonk, NY: IBM Corporation). To evaluate the interobserver variability between the three observers that assessed interbody fusion on CT, the intraclass correlation coefficient (ICC) was calculated, using the Two-Way Mixed model. Intergroup differences (pseudarthrosis versus fusion) were assessed by an independent t-test in case of normality and a Mann-Whitney U-test otherwise. Intraindividual differences (operated versus non-operated segments, endplate versus intervertebral) and intertime differences (six weeks versus one year) were evaluated by a paired samples t-test in case of normality and a Wilcoxon Signed-Rank test otherwise. P-values ≤ 0.05 were used to indicate statistically significant differences. Receiver Operating Characteristic (ROC) curves were used to test the performance of ^{18}F-fluoride PET/CT parameters at six weeks for the prediction of bony fusion one year postoperative. The

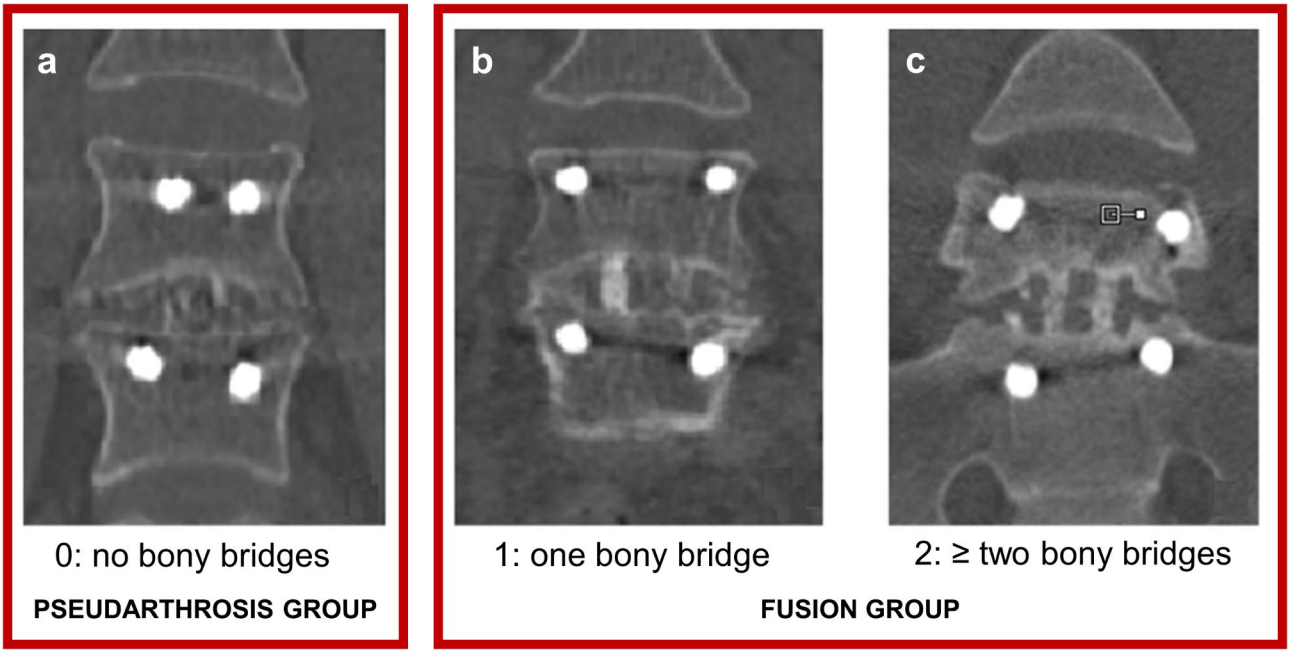

Fig. 2 Examples of interbody fusion scoring on diagnostic CT one year postoperatively and classification into groups. Score 0 (**a**): no bony bridges. Score 1 (**b**): one complete bony bridge within or surrounding the cages, left or right. Score 2 (**c**): two or more complete bony bridges within or surrounding the cages

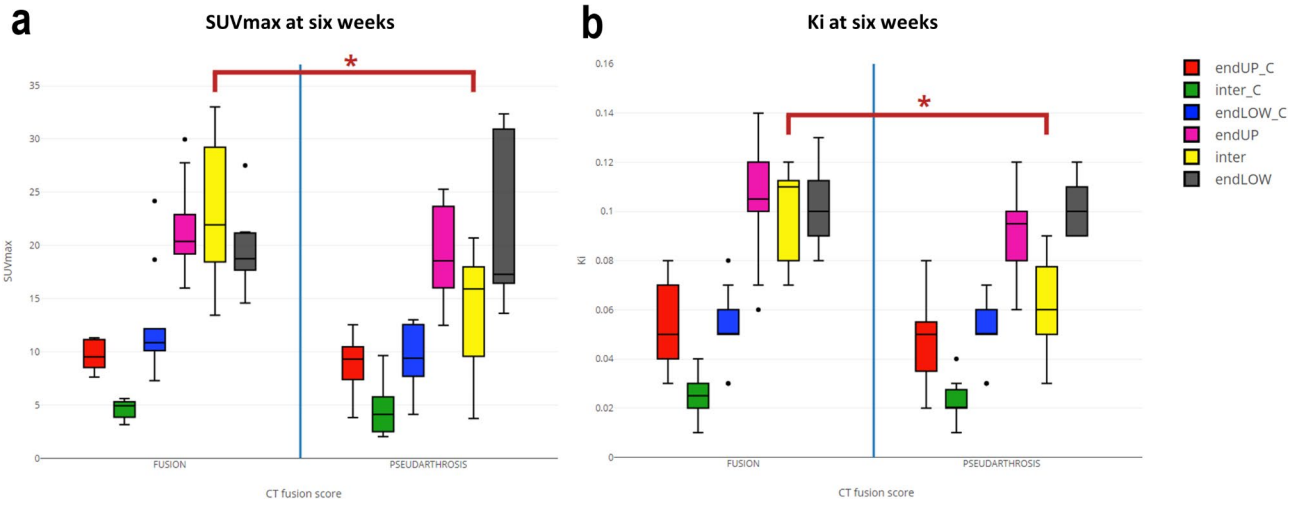

Fig. 3 SUVmax (**a**) and Ki (**b**) at six weeks after PLIF for the fusion group (left from the vertical blue line) and for the pseudarthrosis group (right from the vertical blue line) of the control ROIs (endUP_C, inter_C, endLOW_C in red, green and blue respectively) and the operated ROIs (endUP, inter, endLOW in pink, yellow and grey respectively). Statistically significant differences between the groups were depicted by a red asterisk

Table 2 P-values for the intergroup differences between the fusion group and pseudarthrosis group in SUVmax, Ki, K1/k2, k3/(k2 + k3) at six weeks and one year after PLIF for the six ROIs. A red font was used to indicate p-values ≤ 0.05

	Comparison	6 WEEKS p-values				1 YEAR p-values			
		SUVmax	Ki	K1/k2	k3/(k2 + k3)	SUVmax	Ki	K1/k2	k3/(k2 + k3)
FUSION vs. PSEUDARTHROSIS segments	endUP_C	0.393	0.573	0.813	0.694	0.863	0.0579	0.739	0.218
	inter_C	0.631	0.426	0.461	0.720	0.918	0.654	0.809	0.503
	endLOW_C	0.208	0.918	0.803	0.223	1.000	0.863	0.512	0.468
	endUP	0.315	0.152	0.036	0.175	0.282	0.756	0.605	0.809
	inter	0.005	0.001	0.030	0.173	0.223	0.251	0.387	0.043
	endLOW	0.796	0.552	0.554	0.882	0.074	0.315	0.912	0.447

SUV = standardized uptake value

ROI = region of interest

area under the curve (AUC) was used as accuracy measure covering all possible interpretation thresholds [22]. The Youden Index was used to obtain the cut-point at which each parameter achieved the optimum differentiating ability with an equal weight given to sensitivity and specificity [23, 24].

Results

Interbody fusion scoring on CT

Of the 21 segments evaluated, eleven levels without bony bridges (score 0) were classified as the pseudarthrosis group, and ten levels with one or more bony bridges (score 1 and score 2) were classified as the fusion group. The ICC for the interbody fusion scoring of the three observers was 0.8.

Analysis of ^{18}F-fluoride PET/CT-scans

Analysis of the PET/CT scans yielded four PET parameters for each ROI: SUVmax from the static scan and Ki, K1/k2, k3/(k2 + k3) from the dynamic scan.

Differences between the fusion group and the pseudarthrosis group

Figure 3 shows the differences in bone metabolic parameters SUVmax and Ki between the fusion and pseudarthrosis group six weeks after PLIF. An overview of p-values for intergroup differences is provided in Table 2. SUVmax and Ki of ROI inter were significantly lower in the pseudarthrosis group compared to the fusion group (SUVmax = 13.47 ± 5.88 and SUVmax = 22.59 ± 6.42 respectively, $p = 0.005$; Ki = 0.060 ± 0.02 and Ki = 0.10 ± 0.02 respectively, $p = 0.001$).

When comparing the operated ROIs to the control ROIs, significantly higher SUVmax and Ki values were found in the operated ROIs for both the fusion and the pseudarthrosis group. Focusing on the operated segments, the endplates and the intervertebral disc space were equally metabolically active in the fusion group, while in the pseudarthrosis group the bone metabolic activity of the intervertebral disc space was significantly lower than at the endplates. Focusing on the control segments, the metabolic activity was significantly lower in the intervertebral disc space compared to at the

endplates, similar to the pattern seen in the operated pseudarthrotic segments.

Fig. 4 shows the intergroup differences between parameters related to bone blood flow (K1/k2) and bone mineral incorporation (k3/(k2 + k3)), at six weeks and one year after PLIF.

At six weeks postoperatively, K1/k2 in the operated upper endplate and intervertebral disc space was significantly higher in the fusion group compared to the pseudarthrosis group ($p = 0.036$ and $p = 0.030$ respectively) (Fig. 4a). No intergroup differences were found for k3/(k2 + k3) (Fig. 4b). An overview of the p-values for intra-individual differences for the fusion group at six weeks and one year is provided in Table 3.

When comparing the operated to the control ROIs for the fusion group, significantly higher K1/k2 values were found in all three operated ROIs. While in the pseudarthrosis group K1/k2 was increased in the operated intervertebral disc space only. k3/(k2 + k3) was significantly higher in all three operated ROIs in comparison to the control ROIs for both the fusion and the pseudarthrosis group.

At one year postoperatively, no intergroup differences were found for K1/k2 (Fig. 4c). k3/(k2 + k3) in the operated intervertebral disc space was significantly lower in the pseudarthrosis group compared to the fusion group ($p = 0.043$) (Fig. 4d). K1/k2 and k3/(k2 + k3) values were significantly higher in all three operated ROIs compared to the control ROIs for both the fusion and the pseudarthrosis group, except for K1/k2 in the operated lower endplate of the fusion group. An overview of the p-values

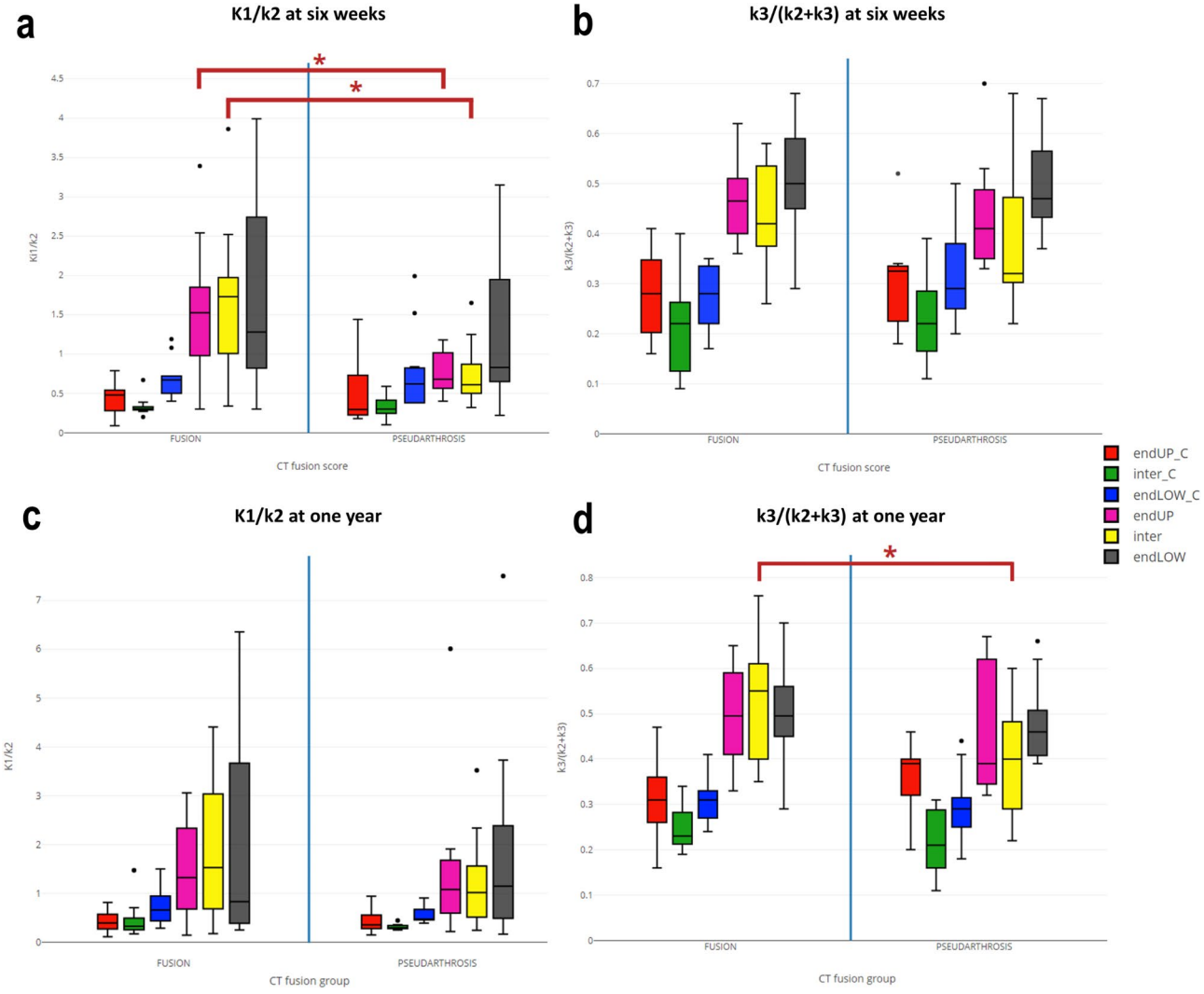

Fig. 4 K1/k2 and k3/(k2 + k3) at six weeks after PLIF (**a** and **b**) and at one year (**c** and **d**), for the fusion group (left from the vertical blue line) and for the pseudarthrosis group (right from the vertical blue line) of the control ROIs (endUP_C, inter_C, endLOW_C in red, green and blue respectively) and the operated ROIs (endUP, inter, endLOW in pink, yellow and grey respectively). Statistically significant differences between the groups were depicted by a red asterisk

Table 3 P-values for the intraindividual differences within the fusion group in SUVmax, Ki, K1/k2, k3/(k2 + k3) at six weeks and one year after PLIF for the operated rois versus the control rois and for the endplate rois versus the intervertebral rois. A red font was used to indicate p-values ≤ 0.05

	Comparison		6 WEEKS p-values				1 YEAR p-values			
			SUVmax	Ki	K1/k2	k3/(k2 + k3)	SUVmax	Ki	K1/k2	k3/(k2 + k3)
FUSION segments	operated ROIs vs. control ROIs	endUP vs. endUP_C	0.005	0.005	0.011	0.028	0.007	0.005	0.005	0.007
		inter vs. inter_C	0.005	0.008	0.008	0.005	0.005	0.005	0.022	0.008
		endLOW vs. endLOW_C	0.007	0.008	0.028	0.008	0.036	0.009	0.333	0.005
	endplate ROIs vs. intervertebral ROIs	endUP_C vs. inter_C	0.005	0.005	0.066	0.063	0.005	0.007	0.575	0.510
		endLOW_C vs. inter_C	0.005	0.005	0.005	0.013	0.005	0.005	0.005	0.021
		endUP_C vs. endLOW_C	0.203	0.799	0.008	0.128	0.386	0.114	0.022	0.508
		endUP vs. inter	0.386	0.441	0.767	0.678	0.646	0.721	0.169	0.047
		endLOW vs. inter	0.203	0.889	0.374	0.314	0.161	0.203	0.721	0.169
		endUP vs. endLOW	0.333	0.594	0.799	0.953	0.401	0.445	0.799	0.646

SUV = standardized uptake value

ROI = region of interest

Table 4 P-values for the intraindividual differences within the pseudarthrosis group in SUVmax, Ki, K1/k2, k3/(k2 + k3) at six weeks and one year after PLIF for the operated rois versus the control rois and for the endplate rois versus the intervertebral rois. A red font was used to indicate p-values ≤ 0.05

	Comparison		6 WEEKS p-values				1 YEAR p-values			
			SUVmax	Ki	K1/k2	k3/(k2 + k3)	SUVmax	Ki	K1/k2	k3/(k2 + k3)
PSEUDARTHROSIS segments	operated ROIs vs. control ROIs	endUP vs. endUP_C	0.005	0.012	0.069	0.017	0.004	0.005	0.017	0.022
		inter vs. inter_C	0.005	0.003	0.005	0.008	0.003	0.003	0.004	0.008
		endLOW vs. endLOW_C	0.005	0.003	0.155	0.003	0.011	0.007	0.028	0.008
	endplate ROIs vs. intervertebral ROIs	endUP_C vs. inter_C	0.005	0.012	0.484	0.017	0.003	0.005	0.074	0.005
		endLOW_C vs. inter_C	0.005	0.003	0.003	0.008	0.003	0.003	0.003	0.003
		endUP_C vs. endLOW_C	0.284	0.484	0.208	0.327	0.594	0.005	0.059	0.012
		endUP vs. inter	0.022	0.003	0.959	0.109	0.008	0.003	0.286	0.051
		endLOW vs. inter	0.028	0.003	0.114	0.026	0.214	0.037	0.139	0.021
		endUP vs. endLOW	0.074	0.086	0.248	0.021	0.214	0.721	0.575	0.214

SUV = standardized uptake value

ROI = region of interest

for intraindividual differences for the pseudarthrosis group at six weeks and one year is provided in Table 4.

In other words, pseudarthrotic patients exhibit lower bone blood flow towards the operated segment in comparison to fused patients at six weeks postoperatively, which seems to be related to less bone mineral incorporation in the intervertebral disc space one year postoperatively.

Level L4-L5 was operated on in 9 patients and level L5-S1 in 12 patients. A t-test showed no differences in any of the variables that were evaluated in the manuscript.

Differences in overall bone metabolism between six weeks and one year

Figure 5 shows the intertime differences in bone metabolism for both the fusion and the pseudarthrosis group. For the fusion group, a significant decrease in bone metabolic activity over time was observed in the upper endplate ($p = 0.005$), intervertebral disc space ($p = 0.005$) and lower endplate ($p = 0.012$) of the operated segment. For the pseudarthrosis group, a significant decrease in bone metabolic activity over time was observed in the operated lower endplate ($p = 0.022$), but not in the upper endplate ($p = 0.575$) nor in the intervertebral disc space ($p = 0.074$). For both groups, the operated ROIs remained significantly higher than the respective control ROIs one year after PLIF ($p = 0.007$, $p = 0.005$, $p = 0.036$ for the upper endplate, intervertebral disc space, lower endplate respectively of the fused segments and $p = 0.004$, $p = 0.003$, $p = 0.011$ respectively for the pseudarthrotic segments).

ROC curves

The ROC curves in Fig. 6 evaluate the effectiveness of SUVmax, Ki, K1/k2 and k3/(k2 + k3) in the operated intervertebral disc space at six weeks to predict bony fusion one year after PLIF. With an AUC of 0.91, Ki had the highest discriminative power, followed by SUVmax (AUC = 0.86), K1/k2 ((AUC = 0.83) and k3/(k2 + k3) (AUC = 0.68). Optimal cut-points for SUVmax and Ki were 18.21 and 0.0750, resulting in sensitivity values of 0.80, 0.90 and specificity values of 0.89, 0.73 respectively.

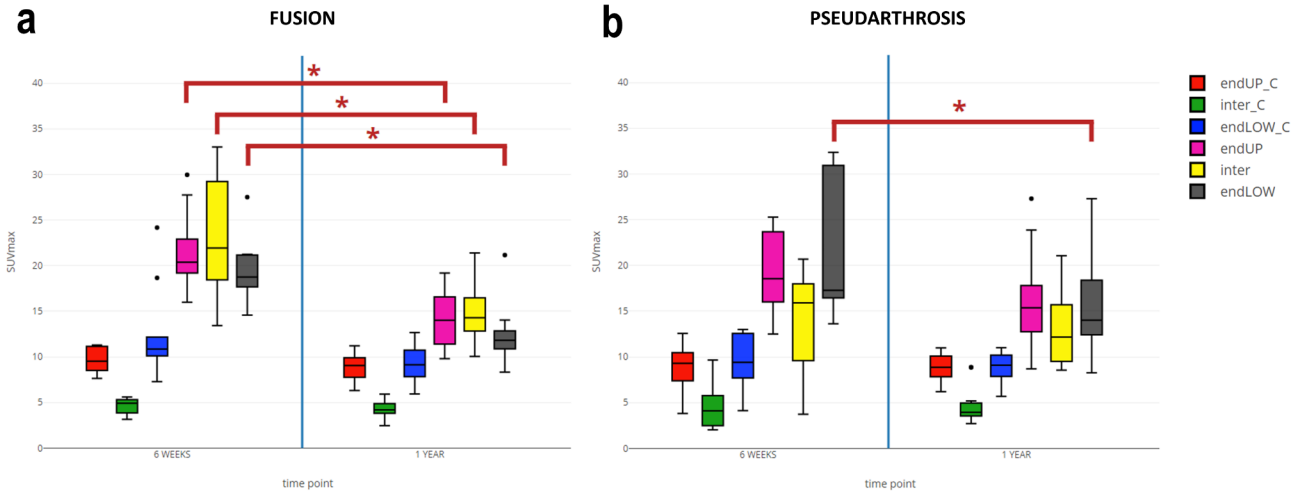

Fig. 5 SUVmax for the fusion group (**a**) and the pseudarthrosis group (**b**) at six weeks (left from the vertical blue line) and at one year after PLIF (right from the vertical blue line) of the control ROIs (endUP_C, inter_C, endLOW_C in red, green and blue respectively) and the operated ROIs (endUP, inter, endLOW in pink, yellow and grey respectively). Statistically significant differences between the groups were depicted by a red asterisk

For K1/k2 and k3/(k2 + k3), optimal cut-points were 0.8750 and 0.3500, resulting in sensitivity values of 0.89, 0.80 and specificity values of 0.90, 0.64 respectively.

Discussion

This prospective study evaluated vertebral bone metabolic activity on ^{18}F-fluoride PET/CT at six weeks and one year after PLIF in relation to bony fusion on CT one year postoperatively.

The most important finding was that six weeks after PLIF, the bone metabolic activity (SUVmax, Ki) in the operated intervertebral disc space was significantly lower in patients who developed pseudarthrosis as compared to patients who attained solid interbody fusion one year postoperatively. In fused segments, the intervertebral bone metabolic activity equals that of the endplates, while pseudarthrotic segments show a pattern of high endplate metabolism and lower intervertebral metabolism, similar to non-operated segments.

Full pharmacokinetic analysis provided deviating patterns between pseudarthrotic and fused segments in parameters related to bone blood flow (K1/k2) and bone mineral incorporation (k3/(k2 + k3)). Pseudarthrotic segments exhibited lower bone blood flow towards the operated segment in comparison to fused segments six weeks postoperatively, which resulted in less bone mineral incorporation in the intervertebral disc space at one year. This may imply that early blood flow to the bone graft, which is crucial for bone fusion to develop in a later stage [25], can be detected with ^{18}F-fluoride PET/CT at six weeks postoperatively.

Dynamic scanning is inherently restricted to a single bed position and therefore a limited field-of view. At the edges of the field-of-view, the measurement uncertainty is larger as the sensitivity decreases towards the edges [26]. This might explain some unexpected findings in the outer ROIs (endUP_C and endLOW). For example, this might explain why K1/k2 in the lower endplate at six weeks was not significantly lower in pseudarthrotic segments compared to fused segments (Fig. 4a).

At six weeks, SUVmax and Ki were superior to K1/k2 and k3/(k2 + k3) in terms of potential effectiveness in predicting bony fusion (Fig. 6). However, as can be seen in Figs. 3 and 6; Tables 2, 3 and 4, the end conclusion in terms of significance is the same for all ROIs for SUVmax and Ki. Therefore, SUVmax could be used in clinical practice for ease of calculation. The more elaborate dynamic modeling technique could be used in research related studies to understand bone physiology in more detail.

The level of bone metabolism in successfully fused segments decreased from six weeks to one year postoperatively, but was still increased compared to non-operated segments. This is consistent with literature showing elevated bone metabolism values within operated bone regions over a course of several years after surgery [5, 27]. In contrast, the level of bone metabolism in pseudarthrotic segments remained equally elevated over time. This is in accordance with findings on impaired graft healing of Brenner et al. [5]. Non-decreased levels of bone metabolism at one year can indicate ongoing bony bridging, but other processes such as subsidence can also elevate bone metabolism values [28]. In this study we did not differentiate between these processes. In Caius et al., 18 F NaF uptake measured one month after posterolateral fusion did not correlate to fusion status and/or clinical parameters at one year follow-up [29]. However, only 4 out of the 18 patients were considered as fused and two different types of graft material were used during surgery, adding an extra confounding factor to the study.

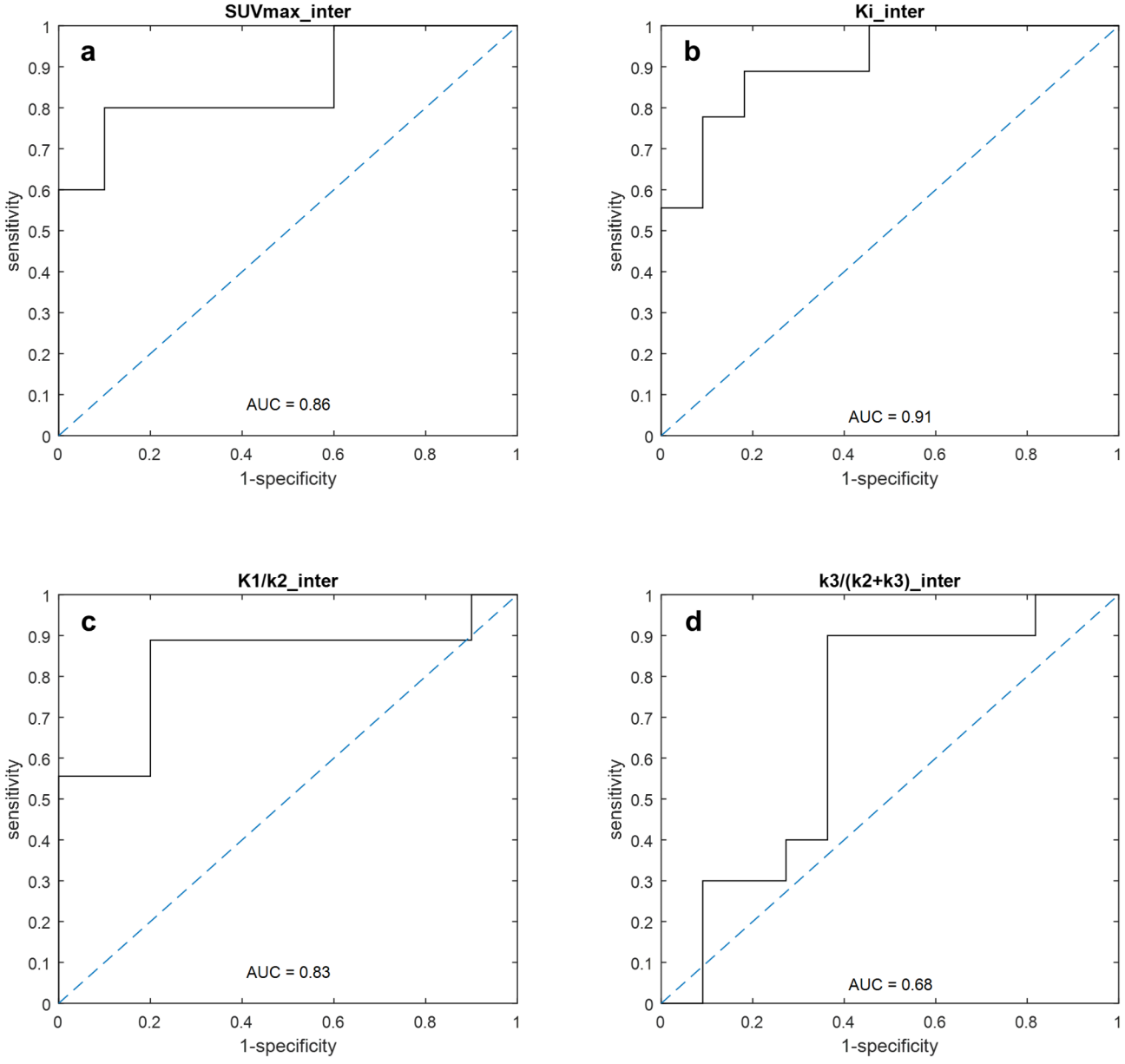

Fig. 6 ROC curves for SUVmax (**a**), Ki (**b**), K1/k2 (**c**), k3/(k2 + k3) (**d**) in the operated intervertebral disc space at six weeks after PLIF to predict fusion at one year. The area under the curve (AUC) is a measure for the diagnostic accuracy. The diagonal dashed line represents the line of equality

A strength of this study was that both fused and pseudarthrotic segments were part of the prospective study cohort. This allowed us to follow-up uncomplicated cases and look for deviations in the pseudarthrosis group. Another strength was the addition of pharmacokinetic modelling to the more commonly used SUV.

A limitation was that the final diagnosis, classifying segments as either fused or pseudarthrotic, was based on CT one year after PLIF. The diagnostic accuracy of CT to diagnose pseudarthrosis is not perfect [4]. However, in absence of the gold standard surgical exploration, for ethical considerations, CT imaging appears to be the most reliable noninvasive method to determine fusion after PLIF [3, 4, 30]. Moreover, in a systematic review, it was shown that fusion assessment on CT was best comparable to surgical exploration as opposed to other noninvasive imaging modalities [31]. CT had the highest odds ratio, indicating it is the most accurate noninvasive imaging modality for the detection of pseudarthrosis after spinal fusion [31]. Furthermore, bony fusion might occur later than one year postoperatively. Together with the strict definition of a bony bridge that was used, this might explain the high level of pseudarthrotic segments observed in this study. An additional follow-up moment several years after surgery would be of value to further differentiate between delayed fusion and definite

pseudarthrosis. We decided not to include clinical outcomes in this manuscript, as this would further complicate the interpretation of the results and overall message, since clinical outcomes and imaging findings do not necessarily correlate. A successful anatomical result after surgery, does not automatically guarantee a pain free patient, neither is an anatomical abnormality necessarily associated with symptoms [3, 32, 33]. Clinical outcomes should be taken into account in a follow-up study. The relatively low resolution of the PET/CT scanner is another limitation. We choose to evaluate relatively large ROIs to minimize the effect of the low resolution. With advancements in technological features of future scanners, the resolution of PET/CT scanning might increase, allowing for smaller ROIs to be evaluated. A higher resolution might make comparison of different areas within the intervertebral disc space feasible.In this study, only 20 patients were included. Our results should be confirmed in larger study cohorts and multi-center studies in order to go towards potential clinical use. In larger study cohorts, more factors that possibly affect the PET/CT signal can be taken into account. For example, whether static PET/CT scanning early after PLIF should be performed in patients that undergo PLIF and are at risk for the development of pseudarthrosis (for example smokers [34] or patients with reduced perfusion). In those cases, aberrant PET/CT findings could hint towards treatment with bone stimulating medication such as novel bone morphogenic proteins, growth hormones, and certain cytokines [35]. Additionally, (dynamic) ^{18}F-fluoride PET/CT could be used as a tool to evaluate bone fracture treatment, consolidation of different bone graft materials and ingrowth of coated prostheses or new cage designs [36] and biomaterials that are new on the market. This manuscript shows an example of a scientific application of PET/CT in spinal fusion patients. With regards to the clinical utility, we would not advise to make PET/CT part of standard clinical practice in these types of patients. We would advise to only use PET/CT in complicated cases where no cause for pain can be found on standard imaging modalities [37] or when testing new graft materials in a research project. The use of SPECT/CT could be an alternative to PET/CT in spinal fusion patients [38–40]. However, Varga et al. stated in a systematic review that there is more evidence to back up the use of PET/CT in spinal fusion as compared to the use of SPECT/CT [41].

To conclude, ^{18}F-fluoride PET/CT six weeks after posterior lumbar interbody fusion provides prognostic information on bony fusion at one year. SUVmax of the operated intervertebral disc space obtained early after PLIF could be useful in clinical practice. Differences between fusion groups in bone blood flow and bone mineral incorporation specifically were demonstrated by full pharmacokinetic modelling.

Author contributions
Study conception and design was performed by Marloes JM Peters and Paul C Willems. Material preparation, data collection and/or analysis were performed by Marloes JM Peters, Roel Wierts, Elisabeth MC Jutten, Wouter AM Broos, Mariel P ter Laak and Paul C Willems. The first draft of the manuscript was written by Marloes JM Peters and all authors commented on previous versions of the manuscript. All authors read and approved the final manuscript.

Funding
An External Research Program grant from Medtronic (Medtronic Bakken Research Center BV) partially covered ^{18}F-fluoride PET/CT scanning costs, Project number: 101025 (ERP grant). Medtronic was not involved in study execution or data analysis.

Data availability
No datasets were generated or analysed during the current study.

Declarations

Ethical approval
This study was performed in line with the principles of the Declaration of Helsinki. Approval was granted by the Ethics Committee of the Maastricht University Medical Center (April 2017 / METC10-1-025).

Consent to participate
Informed consent was obtained from all individual participants included in the study.

Consent to publish
Not applicable.

Competing interests
The authors declare no competing interests.

Received: 4 October 2024 / Accepted: 12 April 2025
Published online: 13 May 2025

References

1. Chan CW, Peng P. Failed back surgery syndrome. Pain Med (Malden Mass). 2011;12(4):577–606.
2. O'Beirne J, O'Neill D, Gallagher J, Williams DH. Spinal fusion for back pain: a clinical and radiological review. J Spinal Disord. 1992;5(1):32–8.
3. Raizman NM, O'Brien JR, Poehling-Monaghan KL, Yu WD. Pseudarthrosis of the spine. J Am Acad Orthop Surg. 2009;17(8):494–503.
4. Choudhri TF, Mummaneni PV, Dhall SS, Eck JC, Groff MW, Ghogawala Z, et al. Guideline update for the performance of fusion procedures for degenerative disease of the lumbar spine. Part 4: radiographic assessment of fusion status. J Neurosurg Spine. 2014;21(1):23–30.
5. Brenner W, Vernon C, Conrad EU, Eary JF. Assessment of the metabolic activity of bone grafts with (18)F-fluoride PET. Eur J Nucl Med Mol Imaging. 2004;31(9):1291–8.
6. Palestro CJ. Radionuclide imaging after skeletal interventional procedures. Semin Nucl Med. 1995;25(1):3–14.
7. Beheshti M, Mottaghy FM, Payche F, Behrendt FF, Van den Wyngaert T, Fogelman I, et al. (18)F-NaF PET/CT: EANM procedure guidelines for bone imaging. Eur J Nucl Med Mol Imaging. 2015;42(11):1767–77.
8. Blau M, Ganatra R, Bender MA. 18 F-fluoride for bone imaging. Semin Nucl Med. 1972;2(1):31–7.
9. Segall G, Delbeke D, Stabin MG, Even-Sapir E, Fair J, Sajdak R, et al. SNM practice guideline for sodium 18F-fluoride PET/CT bone scans 1.0. Journal of nuclear medicine: official publication. Soc Nuclear Med. 2010;51(11):1813–20.
10. Hawkins RA, Choi Y, Huang SC, Hoh CK, Dahlbom M, Schiepers C, et al. Evaluation of the skeletal kinetics of fluorine-18-fluoride ion with PET. Journal of nuclear medicine: official publication. Soc Nuclear Med. 1992;33(5):633–42.
11. Messa C, Goodman WG, Hoh CK, Choi Y, Nissenson AR, Salusky IB, et al. Bone metabolic activity measured with positron emission tomography and [18F] fluoride ion in renal osteodystrophy: correlation with bone histomorphometry. J Clin Endocrinol Metab. 1993;77(4):949–55.

12. Piert M, Zittel TT, Machulla HJ, Becker GA, Jahn M, Maier G, et al. Blood flow measurements with [(15)O]H2O and [18F]fluoride ion PET in Porcine vertebrae. J Bone Mineral Research: Official J Am Soc Bone Mineral Res. 1998;13(8):1328–36.
13. Frost ML, Fogelman I, Blake GM, Marsden PK, Cook G. Jr. Dissociation between global markers of bone formation and direct measurement of spinal bone formation in osteoporosis. J Bone Mineral Research: Official J Am Soc Bone Mineral Res. 2004;19(11):1797–804.
14. Raijmakers P, Temmerman OP, Saridin CP, Heyligers IC, Becking AG, van Lingen A, et al. Quantification of 18F-Fluoride kinetics: evaluation of simplified methods. Journal of nuclear medicine: official publication. Soc Nuclear Med. 2014;55(7):1122–7.
15. Schliephake H, Berding G, Knapp WH, Sewilam S. Monitoring of graft perfusion and osteoblast activity in revascularised fibula segments using [18F]-positron emission tomography. Int J Oral Maxillofac Surg. 1999;28(5):349–55.
16. Peters MJ, Wierts R, Jutten EM, Halders SG, Willems PC, Brans B. Evaluation of a short dynamic 18F-fluoride PET/CT scanning method to assess bone metabolic activity in spinal orthopedics. Ann Nucl Med. 2015;29(9):799–809.
17. Peters M, Willems P, Weijers R, Wierts R, Jutten L, Urbach C, et al. Pseudarthrosis after lumbar spinal fusion: the role of (1)(8)F-fluoride PET/CT. Eur J Nucl Med Mol Imaging. 2015;42(12):1891–8.
18. Wong KK, Piert M. Dynamic bone imaging with 99mTc-labeled diphosphonates and 18F-NaF: mechanisms and applications. J Nuclear Medicine: Official Publication Soc Nuclear Med. 2013;54(4):590–9.
19. Piert M, Zittel TT, Becker GA, Jahn M, Stahlschmidt A, Maier G, et al. Assessment of Porcine bone metabolism by dynamic. J Nuclear Medicine: Official Publication Soc Nuclear Med. 2001;42(7):1091–100.
20. Puri T, Frost ML, Curran KM, Siddique M, Moore AE, Cook GJ et al. Differences in regional bone metabolism at the spine and hip: a quantitative study using (18)F-fluoride positron emission tomography. osteoporosis international: a journal established as result of Cooperation between the European foundation for osteoporosis and the National osteoporosis foundation of the USA. 2013;24(2):633–9.
21. Frost ML, Blake GM, Cook GJ, Marsden PK, Fogelman I. Differences in regional bone perfusion and turnover between lumbar spine and distal humerus: (18)F-fluoride PET study of treatment-naive and treated postmenopausal women. Bone. 2009;45(5):942–8.
22. Eng J. Receiver operating characteristic analysis: a primer. Acad Radiol. 2005;12(7):909–16.
23. Youden WJ. Index for rating diagnostic tests. Cancer. 1950;3(1):32–5.
24. Ruopp MD, Perkins NJ, Whitcomb BW, Schisterman EF. Youden index and optimal cut-point estimated from observations affected by a lower limit of detection. Biometrical J Biometrische Z. 2008;50(3):419–30.
25. Herkowitz HN, Garfin SR, Eismont FJ, Bell GR, Balderston RA. Rothman-Simeone the spine E-Book: expert consult. Elsevier Health Sciences; 2011.
26. Cherry SR, Dahlbom M, editors. PET: physics, instrumentation, and scanners. PET; 2006.
27. Piert M, Winter E, Becker GA, Bilger K, Machulla H, Muller-Schauenburg W, et al. Allogenic bone graft viability after hip revision arthroplasty assessed by dynamic [18F]fluoride ion positron emission tomography. Eur J Nucl Med. 1999;26(6):615–24.
28. Brans B, Weijers R, Halders S, Wierts R, Peters M, Punt I, et al. Assessment of bone graft incorporation by 18 F-fluoride positron-emission tomography/computed tomography in patients with persisting symptoms after posterior lumbar interbody fusion. EJNMMI Res. 2012;2(1):42.
29. Constantinescu CM, Jacobsen MK, Gerke O, Andersen M, Høilund-Carlsen PF. Fusion and healing prediction in posterolateral spinal fusion using (18) F-Sodium Fluoride-PET/CT. Diagnostics (Basel). 2020;10(4).
30. Bahir AW, Daxing W, Jiayu X, Bailian L, Shao G. Comparative efficacy and fusion outcomes of unilateral bi-portal endoscopic transforaminal lumbar interbody fusion versus minimally invasive transforaminal lumbar interbody fusion in treating single-segment degenerative lumbar spondylolisthesis with lumbar spinal stenosis: a two-year retrospective study. J Orthop Surg Res. 2024;19(1):835.
31. Peters MJM, Bastiaenen CHG, Brans BT, Weijers RE, Willems PC. The diagnostic accuracy of imaging modalities to detect pseudarthrosis after spinal fusion-a systematic review and meta-analysis of the literature. Skeletal Radiol. 2019;48(10):1499–510.
32. Heggeness MH, Esses SI. Classification of pseudarthroses of the lumbar spine. Spine (Phila Pa 1976). 1991;16(8 Suppl):S449–54.
33. Rothman RH, Booth R. Failures of spinal fusion. Orthop Clin North Am. 1975;6(1):299–304.
34. Hermann PC, Webler M, Bornemann R, Jansen TR, Rommelspacher Y, Sander K, et al. Influence of smoking on spinal fusion after spondylodesis surgery: A comparative clinical study. Technol Health Care: Official J Eur Soc Eng Med. 2016;24(5):737–44.
35. Dyke JP, Aaron RK. Noninvasive methods of measuring bone blood perfusion. Ann N Y Acad Sci. 2010;1192:95–102.
36. Cofano F, Armocida D, Ruffini L, Scarlattei M, Baldari G, Di Perna G et al. The efficacy of trabecular titanium cages to induce reparative bone activity after lumbar arthrodesis studied through the 18f-Naf PET/CT scan: observational clinical In-Vivo study. Diagnostics (Basel). 2022;12(10).
37. Pouldar D, Bakshian S, Matthews R, Rao V, Manzano M, Dardashti S. Utility of 18F sodium fluoride PET/CT imaging in the evaluation of postoperative pain following surgical spine fusion. Musculoskelet Surg. 2017;101(2):159–66.
38. Pendleton J, Ng A, SPECT/CT Scan. A new diagnostic tool in pain medicine. Curr Pain Headache Rep. 2023;27(11):729–35.
39. Kaiser R, Varga M, Lang O, Waldauf P, Vaněk P, Saur K, et al. Spinal fusion for single-level SPECT/CT positive lumbar degenerative disc disease: the SPINUS I study. Acta Neurochir (Wien). 2023;165(9):2633–40.
40. Tender GC, Davidson C, Shields J, Robichaux J, Park J, Crutcher CL, et al. Primary pain generator identification by CT-SPECT in patients with degenerative spinal disease. Neurosurg Focus. 2019;47(6):E18.
41. Varga M, Kantorová L, Langaufová A, Štulík J, Lančová L, Srikandarajah N, et al. Role of Single-Photon emission computed tomography imaging in the diagnosis and treatment of chronic neck or back pain caused by spinal degeneration: A systematic review. World Neurosurg. 2023;173:65–78.

Publisher's note

Springer Nature remains neutral with regard to jurisdictional claims in published maps and institutional affiliations.